Impact of Spatial Traffic Variation on Energy Savings and Devices Lifetime in Core Networks

Filip Idzikowski*, Frank Pfeuffer†, Axel Werner† and Luca Chiaraviglio‡
*Faculty of Electronics and Telecommunications, Poznan University of Technology, Poland, filip.idzikowski@put.poznan.pl
†Zuse Institute Berlin, Germany, {lastname}@zib.de
‡University of Rome - La Sapienza, Italy, luca.chiaraviglio@uniroma1.it

***Abstract*—Traffic variation heavily impacts energy savings achieved by putting Line Cards (LCs) into Sleep Mode (SM) in core Internet Protocol (IP)-over-Wavelength Division Multiplexing (WDM) networks. We propose a simple traffic model covering temporal and spatial traffic variation and investigate the impact of (controlled) traffic variations on energy savings achieved with the Energy Watermark Algorithm (EWA) as well as on devices lifetime in realistic network scenarios. The results indicate that spatial variation of traffic is no obstacle in saving energy in the networks. We point out the need for consistent routing schemes between the reference network (designed with a sophisticated Mixed-Integer Linear Programming (MILP) formulation in our case) and the solutions computed dynamically during network operation (with the lifetime-unaware EWA in our case).**

I. Introduction

Power consumption in core IP-over-WDM networks has been constantly increasing in the last years. To invert this trend, different approaches, often referred to as "green networking", have been proposed (see, e.g., the surveys [1, 2]). Among the different solutions to reduce power consumption in backbone networks, one of the most promising ones is the application of low power modes to network devices. The main idea of this approach is to deactivate the network resources when they are unused and activate them when needed again. However, frequent changes of the devices' power states tend to have a deteriorating influence on their lifetime. Therefore, a backbone network experiences energy and lifetime variations as a consequence of the activation/deactivation of its resources.

The main process that drives the power state variations is the evolution of traffic over time. More precisely, networks are dimensioned to satisfy the peak traffic demands. However, traffic varies both in space and time. For instance, a residential area may experience high traffic during the evening (when most users are at home), while a business area will be more loaded during the day (when most users are working). During the night very few users generate traffic, resulting in a low utilization of network devices. Moreover, if the network spans across different time zones, the periods of low utilization will not occur at the same time in all regions of the network, but will be shifted across the time zones.

In this context, several questions arise: How to model spatial and temporal traffic variations in a backbone network? What is the influence of both spatial and temporal traffic variations on the energy savings and on the lifetime of devices? How does the difference across time zones affect the results? The goal of this paper is to give answers to such questions. More in depth, we first propose a simple traffic model that captures temporal and spatial traffic variation. We then build a realistic network scenario adopting a real network topology, as well as the traffic variations derived from our model. We run an algorithm to activate/deactivate the network resources in order to compute the possible energy savings and the effect on devices lifetime, which shows the influence of the proposed traffic model on both the energy savings and the lifetime.

Previous work in the literature has mainly investigated the impact of temporal variations of traffic on the energy savings (see particularly [3]). In this work we go two steps further by: (i) considering the impact on the devices lifetime, and (ii) considering the impact of spatial traffic distribution on both lifetime and energy savings. We believe that the presented results can provide fruitful indications on how future networks should be designed in order to be energy-efficient and lifetime-aware. Furthermore, we point out the sophisticated MILP formulation used to design a realistic reference network. It enforces single-shortest-path routing of IP traffic demands over the IP topology in the reference network. We are not aware of any related work assuming such constraints in the design phase of energy-efficient multilayer backbone networks.

The paper is organized as follows. Section II presents related work regarding traffic modeling in the context of green backbone networking. Our traffic model, including both temporal and spatial variations, is detailed in Section III. Section IV describes the network model. The evaluation scenario is detailed in Section V. Results are analyzed in Section VI, and conclusions are drawn in Section VII. Details of the network design MILP formulation can be found in the Appendix.

II. Related work

Even though many traffic models have been proposed in the literature so far, the field of traffic modeling in the context of green core networking is relatively unexplored. The sinusoidal function is usually used as a parametrized model, e.g., [3–12]. Traffic variation in the context of saving energy is the focus only of [3, 4]. The authors propose a model of aggregated traffic taking the set of considered time periods (by default spanning 24 hours) as well as maximum and minimum traffic volumes as parameters. Our model extends them with (sub)sets of time periods when traffic is high, low, increasing, and decreasing. To the best of our knowledge, no previous related

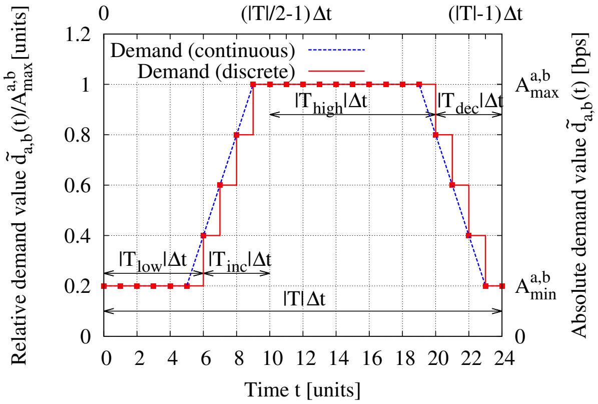

Fig. 1. Temporal traffic model with exemplary relative demand values and even number of elements in the set of time periods T.

work exists that provides a traffic model including parameters to change spatial traffic distribution over time in a controlled way. Some articles consider a shift of traffic according to the time zone in which nodes generating traffic are located (see [13–19]). No variation of spatial traffic distribution is studied in these articles, though. We refer to Table VIII of [2] for a detailed overview of the traffic data used in the research on green core networking.

III. Traffic model

We propose a simple traffic model that allows for capturing and controlling changes of volumes of traffic demands over time as well as changes of the spatial distribution of traffic demands over time. We consider a network with a set of nodes V, and a set of time periods T for evaluation of power consumption during network operation. The length of each time period $t \in T$ is Δt. A traffic matrix $D(t)$ at time period $t \in T$ describes traffic demands between all node pairs in the network. It is composed of elements $d_{a,b}(t)$ containing (directed) traffic demands exchanged between an ordered node pair $(a, b) \in V^2$.

The traffic matrices $D(t)$ for all $t \in T$ are obtained in the following two steps. First, we focus on temporal traffic variation, i.e., all traffic demands follow the same (relative) changes over time, without changes of spatial traffic distribution. In the second step, we add parameters to our model in order to vary spatial traffic distribution over time in a controlled way.

A. Temporal (diurnal) traffic variation

We start out with the assumption that traffic is periodic (day-night pattern) with the period length equal to $|T| \cdot \Delta t$. We distinguish the subsets of time periods $T_{low} \subseteq T$ and $T_{high} \subseteq T$ corresponding to a set of low-demand time periods and a set of high-demand time periods, respectively. Furthermore, we consider linear traffic increase over a set of time periods $T_{inc} \subseteq T$, and linear traffic decrease over a set of time periods $T_{dec} \subseteq T$ as shown in Fig. 1. The traffic demand $\tilde{d}_{a,b}(t)$ between a node pair $(a, b) \in V^2$ is described as:

$$\tilde{d}_{a,b}(t) = \begin{cases} A^{a,b}_{min} & \text{if } t \in T_{low}, \\ \frac{A^{a,b}_{max} - A^{a,b}_{min}}{|T_{inc}|} t + A^{a,b}_{min} + \\ -(A^{a,b}_{max} - A^{a,b}_{min}) \frac{|T_{low}|}{|T_{inc}|} & \text{if } t \in T_{inc}, \\ A^{a,b}_{max} & \text{if } t \in T_{high}, \\ \frac{A^{a,b}_{min} - A^{a,b}_{max}}{|T_{dec}|} t + A^{a,b}_{max} + \\ -(A^{a,b}_{min} - A^{a,b}_{max}) \frac{|T_{low}|+|T_{inc}|+|T_{high}|}{|T_{dec}|} & \text{if } t \in T_{dec}. \end{cases} \quad (1)$$

The model with its parameters allows not only investigation of the influence of the traffic amplitude $(A^{a,b}_{max} - A^{a,b}_{min})$ on network energy consumption, but also the influence of the pace of traffic increase $(A^{a,b}_{max} - A^{a,b}_{min})/|T_{inc}|$ and decrease $(A^{a,b}_{min} - A^{a,b}_{max})/|T_{dec}|$ on network energy consumption.

The traffic demand curve $\tilde{d}_{a,b}(t)$ is different for each node pair $(a, b) \in V^2$ due to the values $A^{a,b}_{max}$ and $A^{a,b}_{min}$. However, we assume in this step that the relative demand $\tilde{d}_{a,b}(t)/A^{a,b}_{max}$ is always the same regardless of the node pair $(a, b) \in V^2$ (compare the primary and the secondary y-axes in Fig. 1). Temporal traffic variation does not change spatial traffic distribution over time if the ratio $A^{a,b}_{max}/A^{a,b}_{min}$ is equal for all traffic demands $\tilde{d}_{a,b}(t)$, and if the sets T_{low}, T_{inc}, T_{high} and T_{dec} are identical for all traffic demands $\tilde{d}_{a,b}(t)$. This is usually not the case in realistic networks, therefore we consider also spatial traffic variation over time in the next step.

B. Spatial traffic variation over time

In order to be able to control the spatial traffic variation over time, we focus on the sets of time periods T_{low}, T_{inc}, T_{high}, and T_{dec}. More precisely, we consider their circular shifting (as explained below), leaving the ratio $A^{a,b}_{max}/A^{a,b}_{min}$ fixed for all $(a, b) \in V^2$ (subject for future work). Wide-range realistic backbone networks often spread over more than one time zone. To account for the temporal shift in traffic due to effects arising from this, we introduce a Time Zone Matrix (TZM)

$$\Theta = \begin{pmatrix} \theta_{0,0} & \cdots & \theta_{0,|V|-1} \\ \vdots & \ddots & \vdots \\ \theta_{|V|-1,0} & \cdots & \theta_{|V|-1,|V|-1} \end{pmatrix}. \quad (2)$$

The value $\theta_{a,b} \in \mathbb{Z}$ for $(a, b) \in V^2$ determines the number of time periods the demand curve for node pair (a, b) has to be shifted temporally due to the fact that a and b lie in time zones differing from a reference time zone. The matrix $\Theta = 0$ is used for a network located completely within the reference time zone.

In order to introduce controlled changes of spatial traffic distribution, we define a Spatial Variation Matrix (SVM)

$$\Gamma = \begin{pmatrix} \gamma_{0,0} & \cdots & \gamma_{0,|V|-1} \\ \vdots & \ddots & \vdots \\ \gamma_{|V|-1,0} & \cdots & \gamma_{|V|-1,|V|-1} \end{pmatrix}, \quad (3)$$

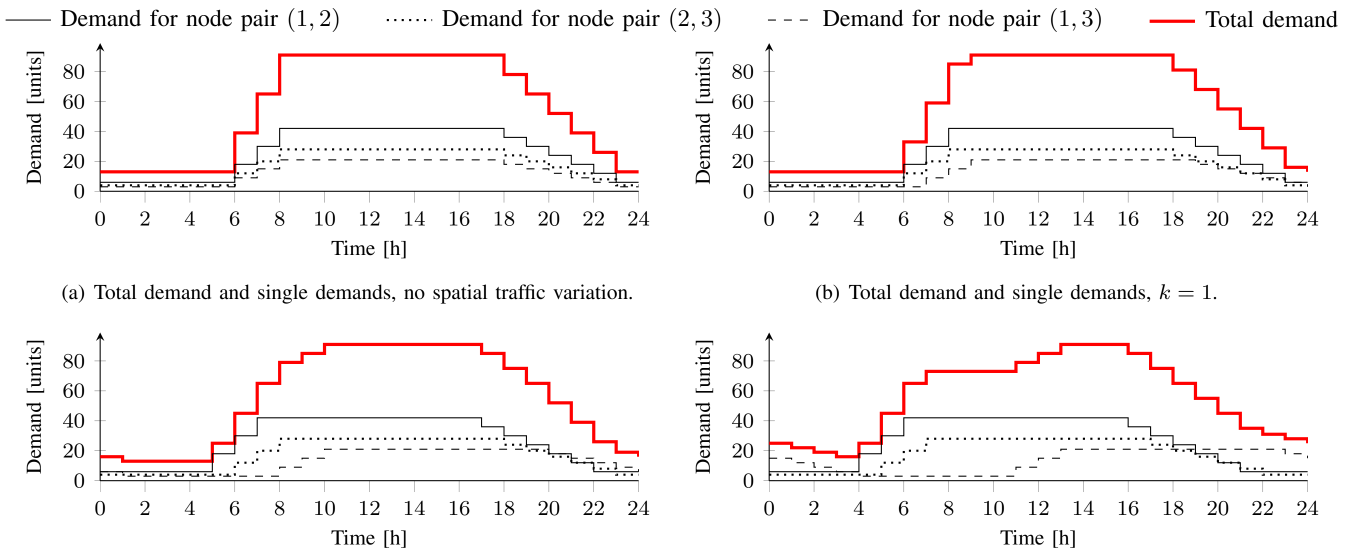

(a) Total demand and single demands, no spatial traffic variation.

(b) Total demand and single demands, $k = 1$.

(c) Total demand and single demands, $k = 2$.

(d) Total demand and single demands, $k = 5$.

Fig. 2. Example for the spatial variation of traffic demands – total network traffic (red) and single demand curves (black) for granularity $\Delta t = 1$ hour and different values of the displacement parameter k in a three-node network.

similarly to the TZM, but with values $\gamma_{a,b} \in [-1, 1]$ for $(a, b) \in V^2$. Additionally, we introduce a time displacement parameter $k \in \{0, \ldots, |T|-1\}$. Then for $(a, b) \in V^2$ the value

$$\zeta_{a,b} = \lfloor k \cdot \gamma_{a,b} \rceil, \tag{4}$$

defines the number of time periods each demand curve should be shifted temporally due to spatial traffic variation[1]. More precisely (and taking into account both $\theta_{a,b}$ and $\zeta_{a,b}$), the spatially varied traffic demand $d_{a,b}(t)$ for $t \in T$ is computed as

$$d_{a,b}(t) = \tilde{d}_{a,b}(t - \theta_{a,b} - \zeta_{a,b} + m \cdot |T|), \tag{5}$$

where the period multiplicity $m \in \mathbb{Z}$ is defined as

$$m = \left\lfloor \frac{t - \theta_{a,b} - \zeta_{a,b}}{|T|} \right\rfloor. \tag{6}$$

Fig. 2 shows the effect of the time displacement parameter k on an exemplary 3-node network with demands for three node pairs (with zero TZM). Initially, these single demands follow curves as defined in Section III-A (discretized), with different values for $A^{a,b}_{max}$ and $A^{a,b}_{min}$ (21, 28, 42 and 3, 4, 6 units, respectively), which results in a total traffic curve of the same type (Fig. 2(a)). For spatial variation, the single demand curves are shifted according to the SVM

$$\Gamma = \begin{pmatrix} 0 & -0.4127 & 1 \\ 0 & 0 & -0.1415 \\ 0 & 0 & 0 \end{pmatrix}, \tag{7}$$

so that for higher values of k the total traffic variation in the network appears as a distorted version of the initial total traffic curve.

[1]The function $\lfloor x \rceil$ stands for rounding of x to the nearest integer value.

IV. Network Model

A. Assumptions

We consider an IP-over-WDM network, i.e., a two-layer network where the layers share a common set of nodes V. In the WDM layer, Optical Cross-Connects (OXCs) at the nodes are interconnected by fiber links that are installed on an undirected physical supply network $G = (V, E)$. Each fiber carries B WDM channels. In the IP layer, IP routers equipped with colored LCs are interconnected by logical links that are established on an undirected logical supply network $H = (V, L)$. Each logical link is realized by one or multiple parallel lightpaths having the same source and target nodes; a lightpath is defined as a WDM channel originating and terminating in the colored LCs and traversing two or more OXCs [20]. It may span multiple fiber links along a path through G (routing over the physical topology), is assigned a unique wavelength[2], and has capacity C bps in both directions. The terminating LCs have also capacity C bps for both transmitting and receiving. Signal regeneration is realized by back-to-back transponders (or colored LCs), what effectively means that a long lightpath is realized by two shorter lightpaths transiting an IP router. No dedicated regenerators are used.

Eventually, traffic (as defined in Section III) arriving at the IP layer has to be routed over the set of logical links from its source node to its target node over the shortest logical path (routing over the logical topology). The network has to provide sufficient lightpath capacity on the involved logical links.

Notation is summarized in Table I in the Appendix.

[2]We assume that the wavelength assignment is done in a post processing step in order to be able to solve the formulated MILP problems.

B. Network design

There is insufficient publicly available data to describe a network of today (including all the installed devices, physical and logical links with their capacities and routing). Therefore it is necessary to design a Static Base Network (SBN) serving as a starting point for the energy evaluation study.

Particularly, we assume that a router n (out of a set of routers N) with capacity R_n can be installed at each node of the network at cost κ_n^{ipr}. Similarly, the cost of installation of an OXC in the network is κ^{oxc}. Installation of (two) LCs associated with a corresponding lightpath costs κ^{lp}. Eventually, cost of fiber installation depends on the length of the corresponding physical supply link $e \in E$.

The SBN is computed using a MILP formulation for a two-layer network design minimizing cost. It builds upon established network design models (see, e.g. [21]), and extends them with constraints on IP traffic routing along single shortest paths through the network of installed logical links in order to be in line with commonly used routing protocols such as Open Shortest Path First (OSPF). This is realized by using node potentials that keep track of routing path lengths. Details of the MILP formulation can be found in the Appendix.

C. Network operation

We assume that the network (with the installed devices according to the SBN) is operated in a dynamic manner. In particular, we use the algorithm called EWA [22] to determine LCs that should be active/inactive in each time period $t \in T$. EWA uses three parameters: W_L, W_H, and ψ. The first two parameters are used to trigger actions to release and establish lightpaths, respectively, in case utilization of the last active lightpath of a logical link is below or above the thresholds W_L and W_H. The last parameter ψ defines the utilization of the last active lightpath on a logical link that should not be exceeded after releasing a lightpath for saving energy.

EWA consists of three phases. It ensures in the first phase that there exists a route between all node pairs with traffic demands. Violation of W_H on any logical link is checked in the second phase, and actions are taken to establish lightpaths in order to stop these violations. Eventually, the lightpaths where W_L is violated are attempted to be released minding that utilization on any lightpath in the network does not increase above ψ. We refer to [22] (and references therein) for implementation details of EWA.

V. Evaluation Scenario

A. Traffic and network

The basis for the parameter settings of the traffic model proposed in Section III is taken from traffic measurements performed on the Abilene network (12 nodes and 15 physical supply links, see [23, 24]). The traffic data covers the period from 2004/03/01 at 00:00 am until 2004/09/10 at 11:55 pm with the granularity 5 min (48096 traffic matrices with 7776 traffic matrices missing in the original data). The same granularity is used in this work ($\Delta t = 5$ min). No newer traffic measurements of the same nature are known to us (see [2, Table VIII]) except for the Géant traffic measurements from 2005 [24, 25].

The maximum and minimum values $A_{min}^{a,b}$ and $A_{max}^{a,b}$ needed for each traffic demand $\tilde{d}_{a,b}(t)$ in the model from Eq. (1) are calculated in the following two steps. First, the following three statistics are computed (for each node pair $(a, b) \in V^2$) out of the 48096 traffic matrices: 20-th percentile, median, and 80-th percentile. Second, means (over all node pairs $(a, b) \in V^2$) of these statistics are used to determine $A_{min}^{a,b}$ (mean of the 20-th percentiles over mean of the medians multiplied by the corresponding median) and $A_{max}^{a,b}$ (mean of the 80-th percentiles over mean of the medians multiplied by the corresponding median).

We use the following parameter settings to generate test traffic matrices. We apply three scaling factors, 229.52, 688.57, and 1147.62 [22] to the original traffic matrices from [24] in order to account for increased traffic demands with respect to the time when the original traffic matrices were captured. This corresponds to 85, 254, and 423 Gbps, respectively, of traffic generated at each node (maximum total demand for the artificially generated sets of traffic matrices).

We assume Greenwich Mean Time (GMT) as the reference time zone. The TZM Θ for the Abilene network is created according to the time zones in which network nodes are located. Five randomly generated SVMs Γ are considered. Eventually, we vary the time displacement parameter $k \in \{0, 1, 6, 12, 24, 36, 48, 72, 96, 120, 144\}$. Note that k corresponds to multiples of Δt, so that, for instance, $k = 24$ yields a maximum time displacement by 2 hours.

We assume that each fiber carries $B = 80$ wavelengths and each wavelength channel has capacity $C = 40$ Gbps. We consider a set of routers N with capacity R_n in the range 640–14720 Gbps. We assume overprovisioning in the SBN design and limit maximum utilization of each lightpath to 50% (i.e., $\delta = 0.5$). Geographical node locations are determined by the corresponding cities (with the two nodes in Atlanta being 2 km away from each other). Lengths of physical links are calculated using the spherical distance between their end-nodes. The maximum lightpath length is set to 3000 km.

B. Capital Expenditure (CapEx) and power

The CapEx cost model based on [26] is used. CapEx of an OXC is assumed to be $\kappa^{\text{oxc}} = 2.75$ units. CapEx of a lightpath with two LCs takes $\kappa^{\text{lp}} = 38.84$ units. Cost of a router κ_n^{ipr} is in the range of 16.67–830.86 units for all routers $n \in N$. Cost of a fiber κ_e^{f} depends on the length of the physical link $e \in E$ (0.0091 units/km and $2 \cdot 10.42$ units contributed by OXCs at both ends of the fiber, and required number of Optical Line Amplifiers (OLAs) and Dynamic Gain Equalizers (DGEs) [27])

EWA targets LCs for energy savings as the most convenient energy-hungry devices to dynamically change power states between SM and Active Mode (AM). We assume that a single (colored) LC consumes 500 W [28] (corresponding to the cost κ^{lp}). Power consumption of a LC in SM is negligible.

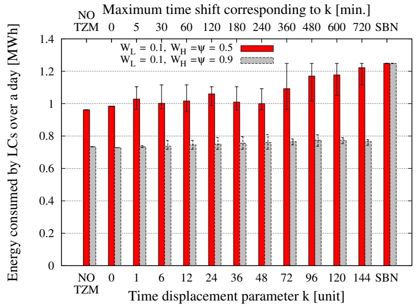

(a) Energy, traffic scaling factor 229.52.

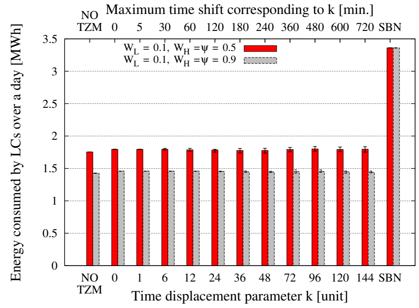

(b) Energy, traffic scaling factor 688.57.

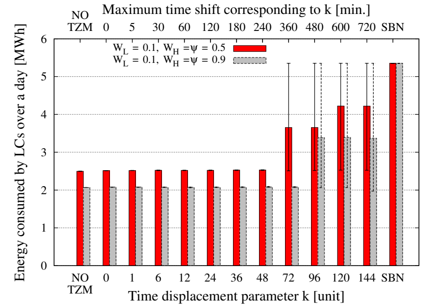

(c) Energy, traffic scaling factor 1147.62.

Fig. 3. Average energy consumed by all LCs over a day over all SVMs in the Abilene-based network using two EWA settings, starting from the SBN designed with the MILP (8) – (17). The error bars indicate the minimum and maximum values over all SVMs.

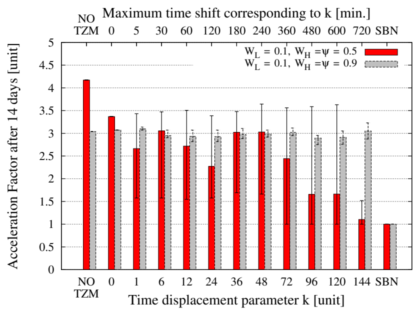

(a) Average AF, traffic scaling factor 229.52.

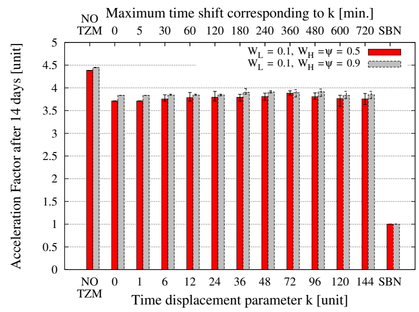

(b) Average AF, traffic scaling factor 688.57.

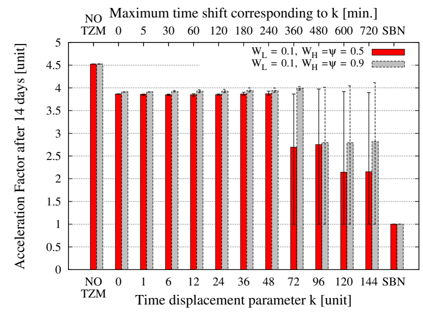

(c) Average AF, traffic scaling factor 1147.62.

Fig. 4. Average AF over all LCs (after 14 days) and over all SVMs in the Abilene-based network using two EWA settings, starting from the SBN designed with the MILP (8) – (17). The error bars indicate the minimum and maximum values over all SVMs.

C. Evaluation Metrics

We use two complementary evaluation metrics. First, we calculate the energy (in Wh) consumed by all active LCs in the network over all time periods in the considered set T. Second, we use the average Acceleration Factor (AF) over all LCs installed in the network to assess devices lifetime. According to [29], the AF takes into account the influence of temperature and temperature variation on the length of devices lifetime. The lifetime can be increased by the fact that a device is in SM (lower temperature than in the AM). However, the process of switching between active and sleep modes induces temperature variations, which reduce the lifetime (see Eq. (3) in [29]). We point out two hardware parameters needed to compute the AF. AF^{sleep} is the ratio between the failure rate of the device dynamically switched between the sleep and active modes and the failure rate of the device always kept in AM (always lower than 1, see [30]). The second hardware parameter, denoted as χ, acts as a weight for the frequency of the active-sleep-active mode cycles [h/cycle]. Values of AF lower than 1 indicate that dynamic usage of SM is beneficial for the devices lifetime. Values of AF greater than 1 indicate that dynamic usage of SM reduces the devices lifetime. In this work we assume AF^{sleep} equal to 0.5 units and χ equal to 0.5 h/cycle [29].

VI. Results

The proposed traffic model and EWA are implemented on a custom-based Java simulation framework. Simulations are performed on a computer with a 64-bit Intel 2.4 GHz CPU and 8 GB RAM. The MILP formulation for SBN design is solved with Cplex [31] using 16 64-bit Intel 2.7 GHz CPUs and 64 GB RAM. Near-optimal solutions were found within a 12-hour time limit with optimization gaps below 1.7%.

We consider two different settings of EWA input parameters: (1) $W_L = 0.1$, $W_H = 0.5$, and $\psi = 0.5$, and (2) $W_L = 0.1$, $W_H = 0.9$, and $\psi = 0.9$. As a consequence, lightpaths are attempted to be released when their utilization is relatively low (i.e., less than 10%). On the other hand, when the lightpath utilization is greater than 50% (90%), additional lightpaths are established in order to avoid network overload. Moreover, the utilization of the last active lightpath on each logical link should not exceed 50% (90%) when a lightpath is released for energy saving.

Given these settings, we run EWA on the considered scenarios (with real TZM Θ) for different values of k, different traffic scaling factors, and 5 randomly generated SVMs. In particular, we choose different values of k between 0 (corresponding to the case in which no time shift is set) and 144 (in which a maximum time shift of 12 hours is enforced). Moreover, we consider the case of zero TZM (i.e., the case when all network nodes are assumed to be located in the same time zone and $k = 0$) denoted as "NO TZM". Additionally, we consider the three traffic scaling factors (229.52, 688.57, and 1147.62) and traffic variation over time as explained in Section V-A. Fig. 3 reports the obtained results in terms of energy consumed by all LCs in the network over a day. Fig. 4 reports the obtained results in terms of average AF over all LCs in the network after 14 days (assuming the same traffic demands on each day). In both cases, averages over all considered SVMs are reported (bar plots) and complemented with the maximum and minimum values (error bars).

Energy consumption, as expected, tends to increase when the traffic scaling factor is increased, see Fig. 3. Interestingly, it is possible to save energy for most values of the time displacement parameter k. This can be clearly observed in the case of a scaling factor 688.57 (Fig. 3(b)). Average energy consumption increases when traffic is scaled with the factor 1147.62 and when k is high (Fig. 3(c)). This is caused by the existence of multiple shortest paths between some node pairs. In particular, EWA sometimes finds other shortest paths than the ones used in the SBN and therefore occasionally has problems with satisfying all the traffic demands (unsatisfied demands never exceed 6%). EWA does not put LCs into SM in such cases, and therefore energy consumption is identical with that in the SBN (compare SBN in Fig. 3(c) with the maximum energy consumption values for $k \geq 72$). This effect of occasional routing incompatibilities is even stronger when the scaling factor is low (see high and intermediate values of k in Fig. 3(a)). On the contrary, it is always possible to save energy when no TZM is used and when k is equal to 0, i.e., when all demands have an off-peak zone occurring during the same hours (cf. Fig. 2(a)) or when the peak times only depend on the time zone where nodes are located.

Furthermore, we confirm that more energy is consumed with the first EWA setting ($W_L = 0.1$, $W_H = \psi = 0.5$) than with the second EWA setting ($W_L = 0.1$, $W_H = \psi = 0.9$). This is due to the fact that with the second setting, the lightpaths can sustain higher utilization.

Considering the average AF (Fig. 4), it is interesting to note that these figures are complementary to the energy figures, i.e., the lower the energy consumption, the higher the AF. The average AF usually takes values between 2.5 and 4.5 meaning that energy saving reduces devices lifetime. For the cases in which EWA encounters routing incompatibilities, the average AF decreases. This happens more frequently with increasing k. In the cases when most LCs are constantly powered on (i.e., the energy consumption of the network using EWA is close to the one of the SBN), few power state reconfigurations are introduced, resulting in an AF close to 1 (see, e.g., the case for $k = 144$ in Fig. 4(c) for $W_L = 0.1$ and $W_H = \psi = 0.5$). Similarly, the AF is equal to 1 in the case of SBN, since no LCs dynamically change power states in the SBN. On the contrary, the highest AF values are reported in the case when no TZM is used. High AF values also occur for low values of k, when also low energy consumption is reported. This shows a trade-off between energy saving and devices lifetime (EWA is an energy-aware, but lifetime-unaware algorithm).

Comparing the AF results of EWA with the two different settings, we point out that lower AF values are achieved with the first (more conservative) setting ($W_L = 0.1$ and $W_H = \psi = 0.5$). However, the relative gains on energy consumption of the second setting are higher than its loss in terms of AF. This can be partially explained by the routing incompatibility issues, which happen more frequently in the case of the first EWA setting (higher overprovisioning results in a higher number of equal-cost routing paths).

VII. Conclusion

We have proposed a simple traffic model covering both temporal and spatial traffic variations. The model has been realistically parametrized and used to generate sets of traffic matrices covering a day with 5-minute granularity. In particular, we varied the spatial distribution of the traffic covered by the generated sets. The sets have been used as input for the energy-aware algorithm EWA, which determines LCs to be put into SM for energy saving.

Our evaluation shows that energy savings are possible when traffic varies over space. In several test instances we have encountered routing incompatibilities between the dynamic EWA solutions and the reference SBN designed with a sophisticated MILP formulation. They occur mainly when spatial traffic variation is high and the load is relatively low. We have found that the energy saving achieved with the lifetime-unaware EWA results in reduced lifetime of LCs experiencing active-sleep-active mode cycles.

As future work, we are going to perform a sensitivity analysis (in terms of energy savings and AF) of the proposed traffic model to its parameters (focusing also on the temporal traffic variation). Moreover, we plan to vary network scenarios, hardware parameters of the devices lifetime model (AF), and consider alternative methods for network design and operation including alternative routing methods and Quality of Service (QoS) metrics.

Acknowledgment

The research leading to these results has received funding from the Polish National Science Center (decision DEC-2014/12/S/ST7/00415), the German Federal Ministry of Education and Research within the SASER project (Safe and Secure European Routing), and the Sapienza Awards DIAMETER (Design and Implementation of Lifetime-Aware Telecommunication Networks). We would like to thank Inken Gamrath, Mickaël Guth, and Ahmad Rostami for their contributions in the initial phase of this work.

Appendix

The MILP formulation for the computation of the SBN is given by (8) – (17) with the notation summarized in Table I. The objective (8) aims at minimizing the installation cost of the network. The constraints (9) model the IP routing as a flow along a single path for each source-destination pair. The constraints (10) allow IP flow only in one direction on installed logical links. The constraints (11) ensure that enough capacity is installed along lightpaths through the physical topology to route the demands of all time periods while respecting a maximum utilization δ of the lightpaths. With constraints (12) and (13) a router module with sufficient capacity to accommodate both backbone and aggregation traffic is chosen, and by constraint (14) a sufficient number of fibers

Minimize cost

$$\min \sum_{i\in V}\Big(\sum_{n\in N}\kappa_n^{\text{ipr}}\,\hat{x}_{i,n}+\kappa^{\text{oxc}}\Big)+\sum_{p\in P}\kappa^{\text{lp}}\,\hat{y}_p+\sum_{e\in E}\kappa_e^{\text{f}}\,\hat{z}_e \tag{8}$$

subject to

$$\sum_{j:\{i,j\}\in L}(\hat{f}_{i,j}^{a,b}-\hat{f}_{j,i}^{a,b})=\begin{cases}1 & \text{if } i=a\\ -1 & \text{if } i=b\\ 0 & \text{otherwise}\end{cases} \qquad \forall i\in V,\,(a,b)\in V^2: a<b \tag{9}$$

$$\hat{f}_{i,j}^{a,b}+\hat{f}_{j,i}^{a,b}\le\hat{\varphi}_{\{i,j\}} \qquad \forall\{i,j\}\in L,\,(a,b)\in V^2: a<b \tag{10}$$

$$\sum_{(a,b)\in V^2:a<b}\frac{1}{\delta}\max\{d_{a,b}(t),d_{b,a}(t)\}\,(\hat{f}_{i,j}^{a,b}+\hat{f}_{j,i}^{a,b})\le\sum_{p\in P_{\{i,j\}}}C\,\hat{y}_p \qquad \forall\{i,j\}\in L,\,t\in T \tag{11}$$

$$\sum_{p\in P_i}C\,\hat{y}_p+\frac{1}{\delta}\max\{d_i^-(t),d_i^+(t)\}\le\sum_{n\in N}R_n\,\hat{x}_{i,n} \qquad \forall i\in V,\,t\in T \tag{12}$$

$$\sum_{n\in N}\hat{x}_{i,n}\le 1 \qquad \forall i\in V \tag{13}$$

$$\sum_{p\in P_e}\hat{y}_p\le B\,\hat{z}_e \qquad \forall e\in E \tag{14}$$

$$\sum_{\{i,j\}\in L}(\hat{f}_{i,j}^{a,b}+\hat{f}_{j,i}^{a,b})\le\hat{\nu}_b^a \qquad \forall(a,b)\in V^2: a<b \tag{15}$$

$$\hat{\nu}_i^a-\hat{\nu}_j^a-1\le(|V|-1)\,(1-\hat{\varphi}_{\{i,j\}}) \qquad \forall i,j\in V:\{i,j\}\in L,\,a\in V \tag{16}$$

$$\hat{\nu}_a^a=0 \qquad \forall a\in V \tag{17}$$

using variables

$$\hat{f}_{i,j}^{a,b},\hat{f}_{j,i}^{a,b},\hat{\varphi}_{\{i,j\}},\hat{x}_{i,n}\in\{0,1\} \qquad \forall i,j,a,b\in V,n\in N$$

$$\hat{\nu}_i^a,\hat{y}_p,\hat{z}_e\in\mathbb{Z}_+ \qquad \forall i,a\in V,p\in P,e\in E.$$

are installed. To abbreviate notation we define the demands emanating and ending at node a at time $t\in T$ as:

$$d_a^+(t)=\sum_{b\in V}d_{a,b}(t) \quad\text{and}\quad d_a^-(t)=\sum_{b\in V}d_{b,a}(t). \tag{18}$$

Then, via (11) and (12) we employ an undirected demand routing scheme, i.e., demand from a source to a target is routed along the same path as demand in the opposite direction, and the necessary capacity along the path has to suffice for the maximum of the demand in each direction. We require that IP traffic is routed along a shortest path through the network of installed logical links. To this end, node potentials $\hat{\nu}_b^a$ are introduced (cf., for instance, [32, Section 7.2]). In general, the offset $\hat{\nu}_a^a$ for $a\in V$ could be any number, while only the difference $\hat{\nu}_b^a-\hat{\nu}_a^a$ matters; due to the constraints (17), $\hat{\nu}_b^a$ can be directly interpreted as the length of the shortest path between a and b (number of logical links). The shortest path routing is then ensured by the constraints (15), which restrict routing path lengths to $\hat{\nu}_b^a$, and the constraints (16), which force the values of $\hat{\nu}_i^a$ and $\hat{\nu}_j^a$ to differ by at most 1, if nodes i and j are connected by a link in the logical topology (indicated by variable $\hat{\varphi}_{\{i,j\}}$ and by the constraints (10)).

References

[1] Y. Zhang, P. Chowdhury, M. Tornatore, and B. Mukherjee, "Energy efficiency in telecom optical networks," *IEEE COMST*, vol. 12, no. 4, pp. 441–458, Fourth Quarter 2010.

[2] F. Idzikowski, L. Chiaraviglio, A. Cianfrani, J. López Vizcaíno, M. Polverini, and Y. Ye, "A survey on energy-aware design and operation of core networks," *IEEE COMST*, Dec. 2015, Early Access.

[3] C. Lange and A. Gladisch, "Limits of Energy Efficiency Improvements by Load-Adaptive Telecommunication Network Operation," in *Proc. CTTE, Berlin, Germany*, May 2011.

[4] ——, "Energy efficiency limits of load adaptive networks," in *Proc. OFC, San Diego, USA*, March 2010.

[5] A. Coiro, M. Listanti, A. Valenti, and F. Matera, "Energy-aware traffic engineering: A routing-based distributed solution for connection-oriented IP networks," *Elsevier ComNet*, vol. 57, no. 9, pp. 2004–2020, June 2013.

[6] Y. Lui, G. Shen, and W. Shao, "Optimal port grouping for maximal router card sleeping," in *Proc. ACP, Guangzhou, China*, Nov. 2012.

[7] Y. Lui, G. Shen, and S. K. Bose, "Energy-efficient opaque IP over WDM networks with survivability and security constraints," in *Proc. ACP, Beijing, China*, Nov. 2013.

[8] Y. Lui, G. Shen, and W. Shao, "Design for energy-efficient IP over WDM networks with joint lightpath bypass and router-card sleeping strategies," *IEEE/OSA JOCN*, vol. 5, no. 11, pp. 1122–11 138, Nov. 2013.

[9] A. P. Bianzino, C. Chaudet, S. Moretti, J.-L. Rougier, L. Chiaraviglio, and E. Le Rouzic, "Enabling sleep mode in backbone IP-networks: a criticality-driven tradeoff," in *Proc. ICC Workshop on Green Communications and Networking, Ottawa, Canada*, June 2012.

[10] A. P. Bianzino, L. Chiaraviglio, M. Mellia, and J.-L. Rougier, "GRiDA: GReen Distributed Algorithm for energy-efficient IP backbone networks," *Elsevier ComNet*, vol. 56, no. 14, pp. 3219–3232, Sep. 2012.

[11] L. Chiaraviglio, M. Mellia, and F. Neri, "Reducing power consumption in backbone networks," in *Proc. ICC, Dresden, Germany*, June 2009.

[12] J. Scharf, "Efficiency analysis of distributed dynamic optical bypassing heuristics," in *Proc. ICC Workshop on Green Communications and Networking, Ottawa, Canada*, June 2012.

[13] X. Dong, T. El-Gorashi, and J. Elmirghani, "Hybrid-power IP over WDM network," in *Proc. WOCN, Colombo, Sri Lanka*, Sep. 2010.

[14] ——, "IP over WDM Networks Employing Renewable Energy Sources," *IEEE/OSA JLT*, vol. 29, no. 1, pp. 3–14, January 2011.

[15] ——, "Energy efficient optical networks with minimized non-renewable power consumption," *AP JNW*, vol. 7, no. 5, pp. 821–831, May 2012.

[16] ——, "Energy-efficient IP over WDM networks with data centres," in *Proc. ICTON, Stockholm, Sweden*, June 2011.

[17] ——, "Green IP over WDM networks with data centers," *IEEE/OSA*

TABLE I
NOTATION USED THROUGHOUT THE PAPER

		Symbol	Description
Parameters	General and MILP	$G=(V,E)$	undirected physical supply network with set of nodes V and set of physical supply links $E \subseteq \{\{i,j\} \subseteq V^2 : i \neq j\}$
		$H=(V,L)$	undirected logical supply network with set of nodes V and set of logical supply links $L \subseteq \{\{i,j\} \subseteq V^2 : i \neq j\}$
		P	set of all (undirected) paths through G on which capacity modules can be installed
		P_i	set of all paths from P where one of the end nodes is $i \in V$
		$P_{\{i,j\}}$	set of all paths from P whose end nodes are the end nodes of $\{i,j\} \in L$
		P_e	set of all paths from P that traverse physical supply link $e \in E$
		N	set of routers that can be installed in the network
		R_n	capacity of router $n \in N$
		C	capacity of a lightpath
		B	number of wavelengths per fiber
		δ	maximum lightpath utilization, $\delta \in (0,1]$
		κ^{oxc}	cost of installing an Optical Cross-Connect (OXC)
		κ^{ipr}_n	cost of installing router $n \in N$
		κ^{lp}	cost of installing a lightpath with Line Cards (LCs)
		κ^{f}_e	cost of installing a fiber on physical supply link $e \in E$
	EWA	AF^{sleep}	ratio between the failure rates of an LC dynamically switched between sleep and active modes and of the LC kept active
		χ	weight for the frequency of the active-sleep-active mode cycles of a LC [h/cycle]
		W_L	threshold on the utilization of the last lightpath on a logical link to trigger attempts to release lightpaths, $W_L \in [0,1)$
		W_H	threshold on the utilization of the last lightpath on a logical link to trigger attempts to establish new lightpaths, $W_H \in (0,1]$
		ψ	maximum utilization of the last lightpath on a logical link, $\psi \in (0,1]$
	Time and traffic	T	set of considered time periods for energy evaluations
		T_{low}	set of low time periods, $T_{low} \subseteq T$
		T_{high}	set of high time periods, $T_{high} \subseteq T$
		T_{inc}	set of time periods with increasing traffic, $T_{inc} \subseteq T$
		T_{dec}	set of time periods with decreasing traffic, $T_{dec} \subseteq T$
		Δt	length of each time period $t \in T$
		$A^{a,b}_{max}$	maximum traffic demand value for the node pair $(a,b) \in V^2$
		$A^{a,b}_{min}$	minimum traffic demand value for the node pair $(a,b) \in V^2$
		$d_{a,b}(t)$, $\bar{d}_{a,b}(t)$	traffic demand between the ordered node pair $(a,b) \in V^2$ during time period $t \in T$ with (without) spatial variation
		$d^+_i(t)$, $d^-_i(t)$	emanating (ending) traffic demand at node $i \in V$ during time period $t \in T$ (Eq. (18))
		Θ	Time Zone Matrix (TZM) with $\theta_{a,b}$ denoting an element of the TZM Θ, $(a,b) \in V^2$
		Γ	Spatial Variation Matrix (SVM) with $\gamma_{a,b}$ denoting an element of the SVM Γ, $(a,b) \in V^2$
		k	time displacement parameter, $k \in \{1,\ldots,\|T\|-1\}$
		$\zeta_{a,b}$	number of time periods by which the demand between nodes $(a,b) \in V^2$ is shifted temporally due to spatial traffic variation
		m	period multiplicity when shifting traffic demands (due to k, $\zeta_{a,b}$, and current $t \in T$, see Eq. (6))
Variables for the SBN		$\hat{f}^{a,b}_{i,j}$	$\in \{0,1\}$ – whether or not the traffic demand from node $a \in V$ to $b \in V$ traverses the logical link $\{i,j\} \in L$ in the direction from $i \in V$ to $j \in V$
		$\hat{\varphi}_{\{i,j\}}$	$\in \{0,1\}$ – whether or not the logical link from $i \in V$ to $j \in V$ is installed (i.e., traversed by any traffic in any direction)
		$\hat{\nu}^a_i$	$\in \mathbb{Z}_+$ – node potential for node $i \in V$ and node $a \in V$, such that $\nu^a_i(t) - \nu^a_a(t)$ is a lower bound for the shortest path from $a \in V$ to $i \in V$ using only installed logical links
		$\hat{y}_p$	$\in \mathbb{Z}_+$ – number of lightpaths established on path $p \in P$
		$\hat{x}_{i,n}$	$\in \{0,1\}$ – whether or not router module $n \in N$ is installed at node $i \in V$; $\hat{x}_{i,n}$ is a variable for Static Base Network (SBN) design and a parameter for evaluations of energy saving during network operation
		$\hat{z}_e$	$\in \mathbb{Z}_+$ – number of fibers installed on physical link $e \in E$; $\hat{z}_e$ is a variable for SBN design and a parameter for evaluations of energy saving during network operation

JLT, vol. 29, no. 12, pp. 1861–1880, June 2011.

[18] X. Dong, A. Lawey, T. El-Gorashi, and J. Elmirghani, "Energy-Efficient Core Networks," in *Proc. ONDM, Colchester, UK*, Apr. 2012.

[19] X. Dong, T. El-Gorashi, and J. Elmirghani, "On the energy efficiency of physical topology design for IP over WDM networks," *IEEE/OSA JLT*, vol. 30, no. 12, pp. 1931–1942, June 2012.

[20] B. Mukherjee, *Optical WDM networks*. Springer, 2006.

[21] A. Betker, I. Gamrath, D. Kosiankowski, C. Lange, H. Lehmann, F. Pfeuffer, F. Simon, and A. Werner, "Comprehensive topology and traffic model of a nationwide telecommunication network," *IEEE/OSA JOCN*, vol. 6, no. 11, pp. 1038–1047, 2014.

[22] E. Bonetto, L. Chiaraviglio, F. Idzikowski, and E. Le Rouzic, "Algorithms for the multi-period power-aware logical topology design with reconfiguration costs," *IEEE/OSA JOCN*, vol. 5, no. 5, pp. 394–410, May 2013.

[23] Y. Zhang, "6 months of abilene traffic matrices," http://www.cs.utexas.edu/~yzhang/research/AbileneTM/, October 2004.

[24] Zuse Institut Berlin, "Library of test instances for Survivable fixed telecommunication Network Design," http://sndlib.zib.de/home.action, 2011.

[25] S. Uhlig, B. Quoitin, J. Lepropre, and S. Balon, "Providing public intradomain traffic matrices to the research community," *ACM SIGCOMM Computer Communication Review*, vol. 36, no. 1, pp. 83–86, 2006.

[26] R. Hülsermann, M. Gunkel, C. Meusburger, and D. A. Schupke, "Cost modeling and evaluation of capital expenditures in optical multilayer networks," *OSA JON*, vol. 7, no. 9, pp. 814–833, 2008.

[27] F. Idzikowski, L. Chiaraviglio, and F. Portoso, "Optimal Design of Green Multi-layer Core Networks," in *Proc. e-Energy, Madrid, Spain*, May 2012.

[28] W. Van Heddeghem and F. Idzikowski, "Equipment power consumption in optical multilayer networks – source data," Tech. Rep. IBCN-12-001-01, Jan. 2012.

[29] L. Chiaraviglio, P. Wiatr, P. Monti, J. Chen, J. Lorincz, F. Idzikowski, M. Listanti, and L. Wosinska, "Is green networking beneficial in terms of device lifetime?" *IEEE COMMAG*, vol. 53, no. 5, pp. 232–240, May 2015.

[30] S. Arrhenius, *Über die Reaktionsgeschwindigkeit bei der Inversion von Rohrzucker durch Säuren*. Wilhelm Engelmann, 1889.

[31] IBM–ILOG, "CPLEX 12.6.0," http://www.ibm.com/software/commerce/optimization/cplex-optimizer/, 2013.

[32] M. Pióro and D. Medhi, *Routing, Flow, and Capacity Design in Communication and Computer Networks*. Morgan Kaufmann Publishers, 2004.